

MATTER ENHANCED NEUTRINO OSCILLATIONS WITH A REALISTIC EARTH DENSITY PROFILE

MARTIN FREUND*

*Institut für Theoretische Physik, Physik-Department, Technische Universität München, James-Frank-Straße
DE-85748 Garching, Germany*

TOMMY OHLSSON†

*Division of Mathematical Physics, Theoretical Physics, Department of Physics, Royal Institute of Technology
SE-100 44 Stockholm, Sweden*

We have investigated matter enhanced neutrino oscillations with a mantle-core-mantle step function and a realistic Earth matter density profile in both a two and a three neutrino scenario. We found that the realistic Earth matter density profile can be well approximated with the mantle-core-mantle step function and that there could be an influence on the oscillation channel $\nu_\mu \rightarrow \nu_\tau$ due to resonant enhancement of one of the mixing angles.

1. Introduction

Step function approximations of the Earth matter density profile have been used by several authors, see *e.g.* Refs. ^{1,2,3,4}, for the analysis of matter effects in neutrino oscillation experiments. In order to investigate the quality of this approximation, we have developed methods to numerically calculate the transition probability amplitudes in a realistic matter density profile. Calculations were performed in a two and a three neutrino framework. The neutrino traveling path length L was divided up into several small intervals. In each of these intervals, in which we assumed constant matter density, we computed the effective mixing parameters. Combining the probability amplitudes of each interval leads to the total probability amplitude from which we obtained the transition probabilities.

We have used three different matter density profiles, two model-like and one realistic: a constant profile just to show the resonance behavior, a step function describing the mantle-core-mantle structure of the Earth, and a realistic Earth density profile ⁵. See Fig. 1 for the different density profiles. For the mantle-core-mantle density profile, we chose $\rho = 5 \text{ g/cm}^3$ for the mantle, $\rho = 12 \text{ g/cm}^3$ for the

*E-mail: martin.freund@physik.tu-muenchen.de

†E-mail: tommy@theophys.kth.se

core, and a core-width equal to half of the Earth's diameter.

In our study we used the mass squared difference as suggested by atmospheric neutrino data from the Super-Kamiokande Collaboration obtained within a two neutrino analysis ⁶

$$\Delta m^2 \simeq 3.2 \cdot 10^{-3} \text{ eV}^2.$$

For the constant density profiles in the case of two neutrino oscillations, we considered the well-known Mikheyev–Smirnov–Wolfenstein (MSW) ⁷ resonance condition

$$\cos 2\theta - \frac{A}{\Delta m^2} = 0, \quad A = A(\rho, E_\nu) = \frac{2\sqrt{2}G_F Y}{m_N} \rho E_\nu, \quad (1)$$

where θ and Δm^2 are the usual mixing parameters for two neutrino oscillations, G_F is the Fermi weak coupling constant, Y ($\simeq 1/2$) is the average number of electrons per nucleon, m_N is the nucleon mass, ρ is the matter density, and E_ν is the neutrino energy. Using Eq. (1) when θ approaches zero, we obtained the resonant energies $E_\nu \simeq 3.6$ GeV for the core and $E_\nu \simeq 8.5$ GeV for the mantle.

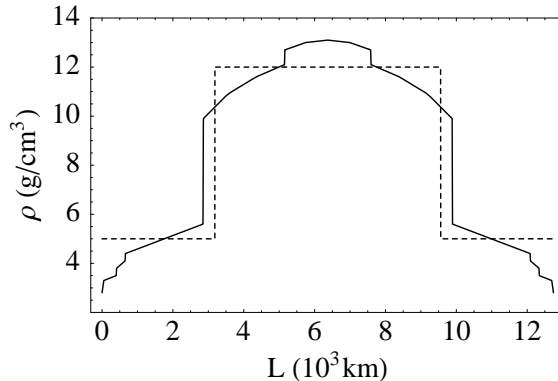


Fig. 1. The matter density profiles. Realistic matter density profile (solid curve) and mantle-core-mantle step function (dashed curve).

2. Two Neutrino Calculation

As mentioned above, we used $\Delta m^2 = 3.2 \cdot 10^{-3} \text{ eV}^2$ for the mass squared difference. Being interested in oscillation enhancement, we chose a small mixing angle $\theta = 0.1$. Using these mixing parameters, we calculated the transition probability $P(\nu_e \rightarrow \nu_x)$, where x could be μ or τ , for neutrinos going through the whole Earth (nadir angle zero). The results for the different matter density profiles discussed above are displayed in Fig. 2 as a function of the neutrino energy E_ν .

In the absence of matter (Fig. 2 (a)), there is a constant maximal probability of $\sin^2 2\theta$ without any enhancement. For constant matter densities (Fig. 2 (b)),

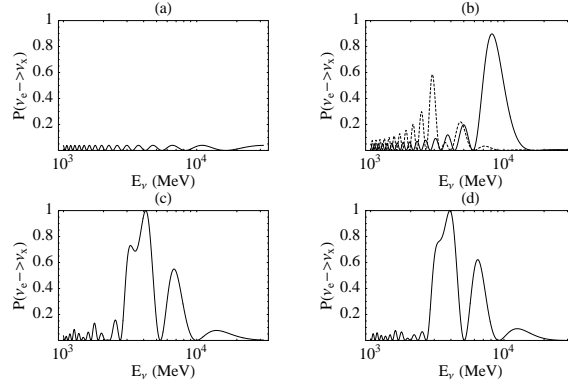


Fig. 2. The transition probability $P(\nu_e \rightarrow \nu_x)$ as a function of the neutrino energy E_ν . (a) zero matter density, (b) constant matter densities (mantle [solid curve] and core [dashed curve]), (c) mantle-core-mantle step function, and (d) realistic Earth matter density profile.

mantle and core, we obtained oscillation enhancements at the expected neutrino energies of $E_\nu \simeq 8.4$ GeV and $E_\nu \simeq 3.5$ GeV, respectively. Figure 2 (c) shows the spectrum for the mantle-core-mantle model. The resonance spectrum is interpreted in the following way^{3,4,8}: The main resonance is due to interference and is therefore not MSW-like. The shoulder to the left on top of the main peak is caused by the core and the peak to the right is caused by the mantle. Both these resonances are typically MSW-like. As seen from Figs. 2 (c)-(d), there is no large qualitative difference between the matter enhancements obtained using the step function and the realistic Earth density profiles. It turns out that the results for the step function profile strongly depend on the widths of the mantle and the core.

The two neutrino model is not suitable for studying matter effects on the $\nu_\mu \rightarrow \nu_\tau$ channel. To obtain more general results, we performed this investigation also in a three neutrino framework.

3. Three Neutrino Calculation

We used a hierarchal mass scheme $\Delta m_{21}^2 \ll \Delta m_{32}^2 \simeq \Delta m_{31}^2$, where the large mass squared difference should describe atmospheric oscillations and the small mass squared difference should be responsible for solar oscillations. As in the two neutrino analysis, we again chose the large mass squared difference as $\Delta m_{32}^2 = 3.2 \cdot 10^{-3} \text{ eV}^2$. The small mass squared difference Δm_{21}^2 was set to zero under the assumption that these transitions play no role at length scales of the diameter of the Earth and smaller.

We also used the standard parameterization for the neutrino mixing matrix with the mixing angles θ_{12} , θ_{13} , and θ_{23} . To accommodate the atmospheric neutrino

result, we chose $\theta_{23} = \pi/4$ giving the following vacuum transition probabilities

$$P(\nu_e \rightarrow \nu_e) = 1 - \sin^2 2\theta_{13} \sin^2 \frac{\Delta m_{32}^2 L}{4E_\nu}, \quad (2)$$

$$P(\nu_e \rightarrow \nu_\mu) = P(\nu_e \rightarrow \nu_\tau) = \frac{1}{2} \sin^2 2\theta_{13} \sin^2 \frac{\Delta m_{32}^2 L}{4E_\nu}, \quad (3)$$

$$P(\nu_\mu \rightarrow \nu_\mu) = 1 - \cos^2 \theta_{13} (2 - \cos^2 \theta_{13}) \sin^2 \frac{\Delta m_{32}^2 L}{4E_\nu}, \quad (4)$$

$$P(\nu_\mu \rightarrow \nu_\tau) = \cos^4 \theta_{13} \sin^2 \frac{\Delta m_{32}^2 L}{4E_\nu}. \quad (5)$$

The parameters relevant for oscillations involving Δm_{32}^2 are θ_{13} and θ_{23} . The magnitude of θ_{12} plays no crucial role even in presence of matter effects. For the numerical calculations we set $\theta_{12} = 0$ but also a maximal angle would not change our obtained results.

Reactor experiments, the solar neutrino deficit and the atmospheric neutrino anomaly all indicate that the mixing angle θ_{13} should be small. The most stringent upper bound of $\sin^2 2\theta_{13} = 0.10$ (valid for $\Delta m^2 > 0.7 \cdot 10^{-3} \text{ eV}^2$) is coming from the CHOOZ experiment⁹. As in the two neutrino calculation we chose $\theta_{13} = 0.1$, which is obviously below the CHOOZ upper bound.

The oscillation probability $P(\nu_e \rightarrow \nu_e)$ is given by an effective two neutrino formula with θ_{13} being the relevant mixing angle. Thus, the two neutrino model discussed above should give a good approximation for the oscillation enhancement obtained in this channel. The resonant energies in the three neutrino model are expected to be approximately the same as calculated in the two neutrino model. This can be seen in Fig. 3 (a), where the oscillation probability $1 - P(\nu_e \rightarrow \nu_e)$ is shown as a function of the neutrino energy E_ν for the realistic Earth density profile. Figure 3 (a) is very similar to the corresponding two neutrino case, see Fig. 2 (d).

From Eq. (3) it can be seen, that in the non-resonant region, electron neutrino disappearance is caused in equal amounts by the transitions $\nu_e \rightarrow \nu_\mu$ and $\nu_e \rightarrow \nu_\tau$. This remains true also in the presence of matter as is shown in Fig. 3 (c).

Due to the resonance enhancement of θ_{13} , we expect a drop in the amplitude for the oscillation probabilities $1 - P(\nu_\mu \rightarrow \nu_\mu)$ and $P(\nu_\mu \rightarrow \nu_\tau)$, see Figs. 3 (b) and (d), respectively. Hence, the oscillation channel $\nu_\mu \rightarrow \nu_\tau$ relevant for the atmospheric neutrino anomaly is influenced indirectly by matter effects through the enhancement of θ_{13} .^a

In similarity to the two neutrino scheme, we found no sizable differences for the mantle-core-mantle model and the realistic Earth matter density profile.

We also investigated the nadir angle dependence in the three neutrino case. The results are shown in Fig. 4 for different nadir angles η . Note that for increasing nadir angle, the resonance for the core shrinks and the mantle starts to dominate the

^aIn two neutrino analyses, the $\nu_\mu \rightarrow \nu_\tau$ oscillation is usually expected not to be influenced by matter effects as there is no coupling to matter via the charged current interactions, which are present only for the electron flavor.

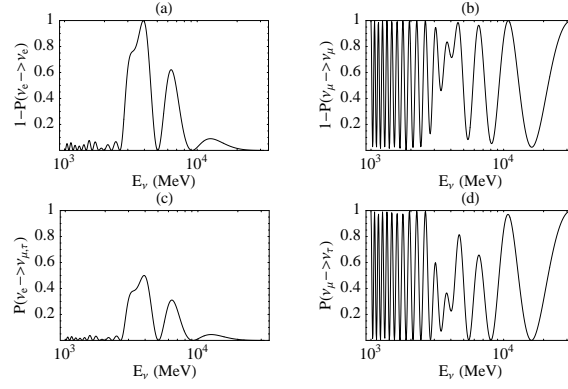


Fig. 3. Different transition probabilities as functions of the neutrino energy E_ν for the realistic Earth matter density profile. (a) $1 - P(\nu_e \rightarrow \nu_e)$, (b) $1 - P(\nu_\mu \rightarrow \nu_\mu)$, (c) $P(\nu_e \rightarrow \nu_{\mu,\tau})$, and (d) $P(\nu_\mu \rightarrow \nu_\tau)$.

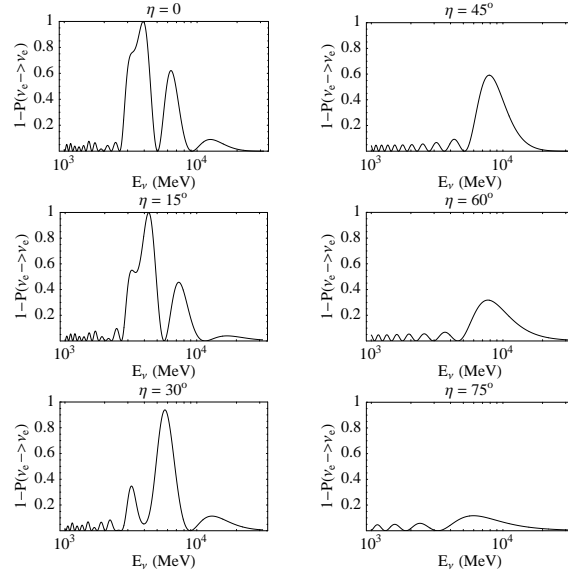


Fig. 4. The probability $1 - P(\nu_e \rightarrow \nu_e)$ as a function of the neutrino energy E_ν for different nadir angles.

resonance spectrum. For angles exceeding $\eta \sim 34^\circ$ neutrinos do no longer traverse the core. The resonance is then centered around the resonant energy $E_\nu \simeq 8.5$ GeV corresponding to the matter density of the mantle (see Fig. 4 for $\eta = 45^\circ$). For larger nadir angles also the mantle resonance fades away due to the fact that the overall traveling path length of the neutrinos in the mantle decreases to zero.

To achieve a large and well defined effect of matter enhancement, we thus propose to further study nadir angles just above the threshold where the traveling length is maximal through the mantle of the Earth.

4. Atmospheric Neutrino Simulation

To describe the quality of the step function approximation in a more intuitive way, we simulated a typical atmospheric neutrino experiment (like the Super-Kamiokande experiment) using the Honda *et al.* atmospheric neutrino fluxes¹⁰. The result is

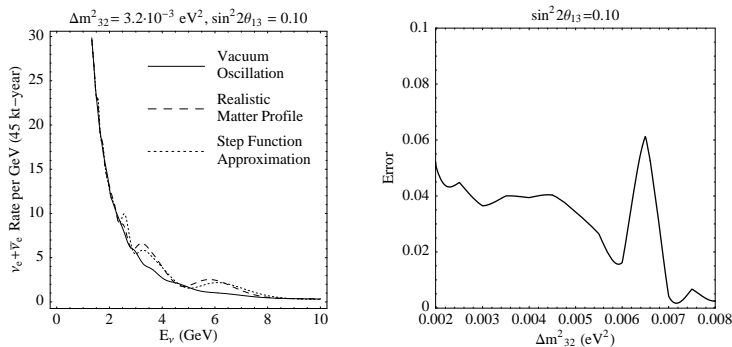


Fig. 5. The left plot shows the energy spectrum of the electron neutrino-like events in an atmospheric neutrino detector for vacuum oscillation (solid), the realistic Earth matter density profile (dashed), and the step function approximation (dotted). The right plot shows the error of the step function approximation for different Δm^2_{32} .

shown in Fig. 5. The left plot shows the energy spectrum of the core-crossing neutrino bin ($\cos \eta = 0.8 \div 1.0$) in a 45kt-detector during one year of running. The figure, which is based on $\sin^2 2\theta_{23} = 1$, $\sin^2 2\theta_{13} = 0.10$, and $\Delta m^2 = 3.2 \cdot 10^{-3} \text{ eV}^2$, shows the cases: vacuum oscillation (solid), realistic matter profile (dashed), and step function approximation (dotted). The enhancements compared to the vacuum case are due to resonant matter effects. The right plot tries to quantify the difference of the two matter profiles. It shows the “error” of the step function approximation in the calculation of the total number of electron neutrino-like events in the core-crossing bin. The error is defined as the ratio $|(N_{\text{RMP}} - N_{\text{SFA}})/(N_{\text{RMP}} - N_{\text{VAC}})|$, where N_{RMP} , N_{SFA} , and N_{VAC} are the total number of events in the core-crossing bin for the realistic matter profile (RMP), the step function approximation (SFA), and vacuum oscillation (VAC), respectively. The defined quantity describes the

error of the step function approximation compared to the absolute magnitude of the matter effects. The error made using the step function approximation is at the level of 5%. Note that the total matter effects in the electron neutrino-like event rate of such an experiment are itself small ($\sim 10\%$). However, future muon storage ring neutrino experiments ¹¹ promise better access to matter effects ¹². With such experiments it will possibly be necessary to take into account details of the matter density profile of the Earth.

5. Summary and Conclusions

We have studied the quality of a mantle-core-mantle step function approximation for the realistic Earth matter density profile in matter enhanced neutrino oscillations. We considered a two neutrino and a three neutrino framework and found that the results given by the model function give an excellent approximation to the results obtained with the realistic profile. The three neutrino analysis we performed, allowed us to investigate effects on the $\nu_\mu \rightarrow \nu_\tau$ channel, which are important for the description of the atmospheric neutrino anomaly. We found a drop of the corresponding oscillation probability in the resonance region. A nadir angle dependent analysis of the enhancement showed that a sizable and clear resonance can be expected for nadir angles around 34° , where the neutrinos spend maximal traveling length in the mantle and do not enter the core. Finally, we tried to quantify the quality of the step function approximation on the level of rates within a simulation of an atmospheric neutrino experiment. The obtained error is at the level of 5%.

Acknowledgments

We are grateful to M. Lindner and H. Snellman for useful discussions as well as S.T. Petcov, E.Kh. Akhmedov, and the Referee for valuable comments and suggestions. This work was supported by the Max-Planck-Institut für Physik (Werner-Heisenberg-Institut) and the Royal Institute of Technology (KTH) Central Internationalization Funds. Support for this work was also provided by the ‘‘Sonderforschungsbereich 375 für Astro-Teilchenphysik der Deutschen Forschungsgemeinschaft’’ and the Engineer Ernst Johnson Foundation. M.F. wishes to thank the Theoretical Physics, KTH for their warm hospitality.

References

1. A. Nicolaidis, *Phys. Lett. B* **200**, 553 (1988).
2. C. Giunti, C.W. Kim, and M. Monteno, *Nucl. Phys. B* **521**, 3 (1998).
3. Q.Y. Liu and A.Yu. Smirnov, *Nucl. Phys. B* **524**, 505 (1998); Q.Y. Liu, S.P. Mikheyev, and A.Yu. Smirnov, *Phys. Lett. B* **440**, 319 (1998); P. Lipari and M. Lusignoli, *Phys. Rev. D* **58**, 073005 (1998); E.Kh. Akhmedov, *Nucl. Phys. B* **538**, 25 (1999); E.Kh. Akhmedov, A. Dighe, P. Lipari, and A.Yu. Smirnov, *Nucl. Phys. B* **542**, 3 (1999); E.Kh. Akhmedov, Report No. hep-ph/9903302, 1999 (unpublished); *Pramana* **54**, 47 (2000) .

4. S.T. Petcov, *Phys. Lett. B* **434**, 321 (1998); **444**, 584(E) (1998); M. Chizhov, M. Maris, and S.T. Petcov, Report No. hep-ph/9810501, 1998 (unpublished); M.V. Chizhov and S.T. Petcov, *Phys. Rev. Lett.* **83**, 1096 (1999); Report No. hep-ph/9903424, 1999 (unpublished).
5. F.D. Stacey, *Physics of the Earth*, 2nd ed. (Wiley, New York, 1977).
6. K. Scholberg [Super-Kamiokande Collaboration], Report No. hep-ex/9905016, 1999 (unpublished).
7. S.P. Mikheyev and A.Yu. Smirnov, *Yad. Fiz.* **42**, 1441 (1985) [*Sov. J. Nucl. Phys.* **42**, 913 (1985)]; S.P. Mikheyev and A.Yu. Smirnov, *Nuovo Cimento C* **9**, 17 (1986); L. Wolfenstein, *Phys. Rev. D* **17**, 2369 (1978); **20**, 2634 (1979).
8. V.K. Ermilova *et al.*, *Short Notices of the Lebedev Institute* **5**, 26 (1986); E.Kh. Akhmedov, *Yad. Fiz.* **47**, 475 (1988) [*Sov. J. Nucl. Phys.* **47**, 301 (1988)]; P. Krastev and A.Yu. Smirnov, *Phys. Lett. B* **226**, 341 (1989).
9. CHOOZ Collaboration, M. Apollonio *et al.*, *Phys. Lett. B* **420**, 397 (1998); **466**, 415 (1999).
10. M. Honda, T. Kajita, K. Kasahara, and S. Midorikawa, *Phys. Rev. D* **52**, 4985 (1995).
11. S. Geer, *Phys. Rev. D* **57**, 6989 (1998); **59** 039903(E) (1999).
12. A. Donini, M.B. Gavela, P. Hernandez, and S. Rigolin, *Nucl. Phys. B* **574**, 23 (2000); T. Ohlsson and H. Snellman, *J. Math. Phys.* **41**, 2768 (2000); V. Barger, S. Geer, R. Raja, and K. Whisnant, Report No. hep-ph/9911524, 1999 (unpublished); T. Ohlsson and H. Snellman, *Phys. Lett. B* **474**, 153 (2000); M. Freund, M. Lindner, S.T. Petcov, and A. Romanino, Report No. hep-ph/9912457, 1999 (unpublished); V. Barger, S. Geer, R. Raja, and K. Whisnant, Report No. hep-ph/0003184, 2000 (unpublished); M. Freund, P. Huber, and M. Lindner, Report No. hep-ph/0004085, 2000 (unpublished).